HHS Public Access

Author manuscript

Int J Pediatr Otorhinolaryngol. Author manuscript; available in PMC 2017 September 01.

Published in final edited form as:

Int J Pediatr Otorhinolaryngol. 2016 September ; 88: 74–81. doi:10.1016/j.ijporl.2016.06.049.

Morphological Changes in the Round Window Membrane Associated with *Haemophilus influenzae*-Induced Acute Otitis Media in the Chinchilla

Shangyuan Jiang[1], **Thomas W. Seale**[2], and **Rong Z. Gan**[1]

[1]School of Aerospace and Mechanical Engineering and Biomedical Engineering Center, University of Oklahoma, Norman, OK

[2]Department of Pediatrics, University of Oklahoma Health Sciences Center, Oklahoma City, OK

Abstract

Objective—The round window membrane (RWM) encloses the round window, the opening into the scala tympani (ST) from the middle ear. During the course of acute otitis media (AOM), structural changes of the RWM can occur that potentially affect sound transmission into and out of the cochlea. The relationship between such structural changes and conductive hearing loss during AOM has remained unclear. The focus of the current study was to compare the thickness distribution across the RWM surface between normal ears and those with AOM in the chinchilla. We the occurrence of AOM-associated histological changes in this membrane compared to uninfected control animals after AOM of two relatively short durations.

Material and methods—AOM was induced by transbullar injection of the nontypeable *Haemophilus influenzae* strain 86-028NP into two groups of adult chinchillas (n=3 each). Bullae were obtained from the two infected groups, at 4 days or 8 days post challenge. Structures and thickness of these RWMs were compared between the two infected treatment groups and to RWMs from uninfected control animals (n=3) at seven different RWM locations.

Results—RWM thickness in infected chinchillas increased significantly at locations along the central line on the 4th day post bacterial challenge compared to values found for uninfected control animals. Lymphocyte infiltration and edema were the primary contributors to these thickness increases. No significant further increases in RWM thickness were observed when RWMs from chinchillas ears infected for 4 and 8 days were compared. Thickness and structural changes at the RWM lateral and medial areas were less visually obvious and not statistically significant among the three treatment groups. These latter RWM regions clearly were less affected during AOM than the central areas.

Corresponding author: Rong Z. Gan, Ph.D. Professor of Biomedical Engineering, School of Aerospace and Mechanical Engineering and Biomedical Engineering Center, University of Oklahoma, 865 Asp Avenue, Room 200, Norman, OK 73019, Phone: (405) 325-1099, Fax: (405) 325-1088, rgan@ou.edu.

Conclusions—This histological study establishes that *H. influenzae*-induced AOM causes significant acute changes in chinchilla RWM structure that are characterized by region-specific increases in thickness. Our new morphological findings comparing normal and diseased chinchilla RWMs identify yet another biomechanical mechanism by which nontypeable *H. influenzae* may contribute to hearing loss in AOM.

Keywords

acute otitis media; round window membrane; histology; *Haemophilus influenzae*; chinchilla

1. INTRODUCTION

The round and oval windows are the two openings from the middle ear that directly connect the middle ear and cochlea. The round window membrane (RWM) covers the round window and vibrates with a phase opposite to the vibration of the stapes at the oval window. The structure of the RWM consists of three layers: an outer epithelial layer facing the middle ear, a core comprised of connective tissue, and an inner epithelial layer facing the scala tympani (ST) [1–5]. Compliance of the RWM affects its ability to be displaced by fluid inside the cochlea, which has a major impact on the transmission of sound into the cochlea [1, 4, 6, 7]. Previous studies have revealed that the RWM also functions as a channel for the transmission of specific substances between the middle ear and the cochlea [1–5, 8]. The mechanical properties and permeability of the RWM are closely associated with its morphology, especially the thickness of the membrane [6, 7].

Acute otitis media (AOM), the most commonly diagnosed disease among young children, is typically caused by bacterial invasion of the middle ear and can result in temporary or permanent hearing loss. Structural changes in the soft tissues of the middle ear, e.g. the tympanic membrane (TM), the stapedial annular ligament and the RWM, contribute significantly to conductive hearing loss induced by AOM [9–13]. A number of published studies have described the morphology of both the healthy and diseased RWMs. These studies include ones involving humans [14, 15] and various clinically relevant animal models such as cats [16, 17], chinchillas [18–23] and guinea pigs [11, 24, 25]. However, the orientation of most of these studies is largely histopathological. There are no published data describing the quantitative measurement of the thickness distribution across RWM surfaces in either normal or AOM ears. The occurrence of thickness changes in the RWM during the course of AOM remains undescribed. Since the stiffness and permeability of the RWM are likely to be dependent on its thickness, a systematically obtained data set describing the thickness distribution of both normal and diseased RWMs is crucial for detailed biomechanical analyses of RWM structure-function relationships [6, 7].

The broad aim of the present study was to begin to fill this important gap in knowledge relevant to hearing loss during acute otitis media caused by the bacterium, *Haemophilus influenzae*. Nontypeable (acapsular) *H. influenzae* is now the most frequent cause of acute otitis media. Previously our research team has investigated the mechanism by which this bacterium alters the microstructure and functions of middle ear soft tissues in the chinchilla model of AOM [12]. Recently we described the occurrence of significant *H. influenzae*-

induced microstructural changes in the chinchilla TM. Such changes included inflammatory cell infiltration into the membrane, cell hyperplasia and edema [13]. As an extension of the previous research, the focus of the present study was to describe how *H. influenzae*-induced infection of the middle ear alters the structure of the RWM.

2. MATERIAL AND METHODS

2.1 The chinchilla AOM model

Nine adult chinchillas (*Chinchilla laniger*) of mixed gender weighing 600–800 g were utilized in this study. These animals were purchased from a USDA approved vendor, Moulton Chinchilla Ranch, Rochester, MN. The protocol for the experiments was approved by the Institutional Animal Care and Use Committee of the University of Oklahoma and met the guidelines of the National Institutes of Health. All animals were examined by otostoscopy before infection to assure that their ears were free from disease prior to administration of nontypeable *H. influenzae*.

Animals were divided into three groups (3 animals for each): untreated control, AOM of 4 days post bacterial challenge, and AOM of 8 days post challenge. AOM was established by bilateral transbullar injection of nontypeable *H. influenzae* strain 86-028NP (a low passage number human clinical isolate) suspended in sterile phosphate buffered saline. The bacterial culture protocol followed the procedure described by Morton et al. [26]. Under general anesthesia (10 mg/kg ketamine and 2 mg/kg xylazine), 0.3 ml of a bacterial suspension containing 3,000 CFU of *H. influenzae* was injected into the superior bulla with a 1 ml syringe equipped with a 26 gauge needle. After the bacteria challenge dose was administered, daily otoscopic examination and animal body temperature measurements were conducted until the animals were euthanized (by Euthasol injection). The uninfected control group was euthanized in the same manner.

2.2 Histological preparation

On either the 4th or 8th day post bacterial challenge, animals were deeply anesthetized by an overdose of ketamine (100mg/kg) and xylazine (20mg/kg). Then a multiple-frequency tympanometer (MAICO MI24, MAICO Diagnostics, Eden Prairie, MN) and an otoscope were used to confirm the presence of AOM in the two infected groups of animals and that the ears of control animals remained uninfected. All animals, including the untreated controls, were then perfused intracardially with fixative (4.0% paraformaldehyde in 0.1 M phosphate buffer, pH 7.2) [27]. The bullae were harvested immediately and then were opened widely. The cochlear apex and the middle ear superior and inferior bony walls were removed to fully expose the RWM to fixative. The bullae then were immersed in fixative overnight at room temperature. On the following day, the bullae were removed from the fixative, placed into phosphate buffered saline solution, and subsequently washed in phosphate buffered saline. These specimens then were decalcified with 10% ethylene diamine tetra acetic acid (EDTA) for 8–10 days. The EDTA solution was replaced daily with fresh solution. When calcium was no longer discernable in the EDTA wash solution, the decalcification process was terminated. Then the ossicular chain of the bulla was separated at the incudostapedial joint with a #11 surgical blade. The cochlea, with its intact RWM, was

dissected from the bulla. Thereafter, specimens were dehydrated in a graded series of ethanol solution and subsequently were decolored in xylene.

2.3. Specimen embedding and sectioning

Upon completion of dehydration step, the RWM specimens were removed from xylene, placed into molten paraffin at a temperature of 54 °C, and incubated at this temperature overnight. On the following day, these specimens were immersed in fresh molten paraffin to remove any remaining xylene. The RWMs then were embedded in new paraffin at an orientation such that the plane of sectioning was approximately perpendicular to the short axis of the RWM and parallel to the long axis. After the paraffin solidified, each specimen was sectioned (8 μm in thickness) from the lateral end to the medial end. These sections were mounted sequentially on glass slides, stained with hematoxylin-eosin, and coverslips were applied.

2.4 Image selection, thickness measurement, and statistical analysis

A Nikon E-800 optical microscope was used to examine and photograph the histologic sections. The microscope was calibrated with a standard calibration slide before measurements were made. Particular attention was given to the thickness of the RWM. Initially, an overview of RWM was captured at lower magnification. The orientation and position of seven target sites used for our membrane thickness measurements are indicated in Fig. 1A. A central line of the RWM from the anterior to posterior (Fig. 1A) was determined by identifying the histologic section that had the longest membrane cross section. Five of the seven locations (A2, A1, O, P1, and P2 shown in Fig. 1A), starting from the anterior region and proceeding to the posterior region of the round window, were evenly distributed along the central line. Locations L and M were selected 0.2 mm laterally and medially, respectively to the center point O. Membrane thickness at each location was determined by averaging the measured values of 4 nearby points within an approximate distance of 150 μm as shown in Fig. 1B. At each of the noted sites or locations, one-way AONVA and Tukey's Honest Significance Tests were used to determine whether the thickness differences at the various locations were statistically significant between the treatment groups. A p value <0.05 was taken as significant for both statistical tests. Note that only the left ears were selected for thickness measurement along different locations to avoid the variations between the left and right ears.

3. RESULTS

3.1 RWM overview

Representative cross-section images of the RWM along its central line are shown at low magnification in Fig. 2. The upper side of the membrane faces the middle ear cavity (MEC) and the lower side of the membrane faces the ST. The five locations selected for thickness measurements are indicated along the membrane from the anterior side on the left to the posterior side on the right.

As shown in Fig. 2A, the control (normal) chinchilla RWM exhibits a smooth convexity toward the cochlear ST. The membrane is thicker at the boundary and thinner at its center.

The edge of the RWM, where the membrane connects to the bony wall of the middle ear, thickens rapidly and forms a fan-shape area between the membrane and bony rim. Little difference in thickness was noted across sites A2 to P2 at this magnification. As seen in these cross sections, the bony boundaries of the RWM are not exactly symmetrical.

Localized irregularities in shape, such as those shown in the cross-section image of the RWM at 4 days post infection (Fig. 2B), suggest that membrane tension may change during the course of AOM. Overall, membranes from chinchillas in both the 4 days and 8 days infected groups are thicker than those in the uninfected control group. Evidence of edema is seen at the RWM boundaries at both its anterior and posterior ends. The middle ear mucosa, continuous with the outer layer of the RWM, exhibits inflammatory cell infiltration and submucosal edema. Inflammatory cells also can be seen inside the ST of cochlea of infected animals but not of uninfected control animals.

A histologic image of the long axis of the RWM at 8 days post challenge is shown in Fig. 2C. More severe alterations in the RWM can be seen at this later time post infection than were observed at 4 days after infection. While thickness differences between the RWMs after 4 and 8 days post infection were not obvious, marked edema clearly can be observed at the boundaries and in the middle ear mucosa of the RWM eight days after infection. Inflammatory cells also are apparent in the inner ear at this later time. Desquamation of a portion of the inner epithelium layer from the middle layer of RWM was associated with persistent middle ear inflammation at this later time post challenge.

3.2 Structure of the RWM center (Location O)

Morphology and thickness of the RWM at its center (location O) in normal controls and in both treatment groups also were examined at higher magnification. These images are shown in Fig. 3. As expected, the uninfected chinchilla RWM (Fig. 3A) is composed of three layers. The outermost layer, which faces the MEC, consists of a single layer of epithelial cells. The middle (fibrous) layer, a core of connective tissues containing fibroblasts, collagen and elastic fibers, makes the greatest contribution to the thickness of the RWM at its center. This layer appears to be the major stress bearing structure of the RWM. Thus, the mechanical properties of RWM are likely to be largely dependent on the microstructure of this middle layer. The innermost layer, which lines the inner ear and faces the ST, consists of a single layer of squamous epithelial cells. This layer exhibits a sparse, less complex structure with larger intracellular spaces compared to the outer layer. RWMs from the ears of each of the uninfected adult chinchillas exhibited these highly similar, triple-layer structures.

Upon infection of the chinchilla middle ear with *H. influenzae*, marked histological changes in RWM structure occurred by the 4th day post challenge (Fig. 3B). The triple-layer structure shown in Fig. 3A remained grossly unchanged. However, proliferation of the epithelial cells occurred and resulted in a denser outer epithelial layer compared to that seen prior to infection. Edema occurred in inter-layer regions and inside the fibrous core. Inflammatory cells including neutrophils, especially leukocytes, clearly infiltrated the fibrous layer. These pathological changes resulted in the marked thickening of the middle layer. The sparse single layer organization of the cells remained unchanged except for the infiltration of neutrophils.

Typical images of the RWM on the 8th day after post *H. influenzae* inoculation are shown in Fig. 3C. Swelling of the outer epithelium and the fibrous layer was similar to that observed in 4-day RWMs. Cell proliferation in the outer epithelial layer led to a closely connected single layer of cells that increased the thickness of the RWM. Edema, which contributed to swelling of the fibrous layer, appeared larger than that observed in images at 4 days post challenge. Persistent middle ear infection over the eight-day period also was associated with the desquamation of the inner epithelial layer in some regions. Neutrophil infiltration was present in all three layers. As a consequence, RWMs from chinchillas infected for 8 days are thicker than those of uninfected chinchillas. However, the duration of the infection (4 and 8 days prior to sacrifice of the animal) is not associated with a statistically significant change in infection severity as measured by these histological outcomes (Table 1).

3.3 Structure of RWM in the areas adjacent to the center (Locations A1, P1, L, and M)

Points A1 and P1 represent two locations along the RWM centerline and 0.2 mm anterior (A1) or posterior (P1) to the center (O). L and M are locations ~0.2 mm, respectively, lateral or medial to the center (O) of the RWM. Representative histologic images of sections in normal, 4 day and 8 day AOM ears at A1 and P1 are shown in Fig. 4. Comparable images at sites L and M are shown in Fig. 5.

In normal ears (upper panels in Figs. 4 and 5), the three-layer structure of the points A1, P1, L, and M is similar to those at the center (O) and to each other. The cell distribution in the upper and inner epithelium layers was slightly less dense at sites A1 and P1 when compared to points O, L and M. In the 4-day and 8-day infected groups (shown in the middle and bottom panels of Figs. 4 and 5), cell proliferation resulted in a dense layer of epithelial cells in the outer layer towards the MEC. Infection-induced edema and neutrophil infiltration inside the membrane also were observed. The thickness of the RWM increased compared to that of controls, but there was no significant thickness variation of the RWM between the 4-day and 8-day infected ears. It is also noted that the RWM thickness at location M seemed thicker than that at locations L, A1, and P1 in both control and infected RWMs. This may suggest that the lateral and medial sides of the RWM are not as symmetric as the anterior and posterior sides. Neither the thickness nor the severity of the inflammation was further changed from 4 days to 8 days post bacterial challenge at all four locations adjacent to the center. Thickness data measured from the RWMs are listed in Table 1.

3.4 Structure of the RWM near the boundaries (Locations A2 and P2)

The images shown in Fig. 6 were obtained from locations ~0.2 mm away from the bony boundary. This is a transitional zone between the fan-shaped boundary and the body of the membrane (Fig. 2). Histologic images from locations A2 and P2 identify structural variations in proximity to the anterior and posterior boundary in normal and AOM ears. A2 and P2 are locations at the anterior and posterior boundary, respectively. As can be seen in upper panels of Fig. 6, the thickness of the RWM was not uniformly distributed as that at the central area in uninfected ears. The membrane thickened near the boundaries. In the middle panel of Fig. 6, the cellular proliferation, edema and cell infiltration in the fibrous layer appeared 4 days after infection and consequently, the membrane was thicker 4 days after

infection. The inflammatory response as well as the membrane thickness did not exhibit significant changes between the 4th days and 8 days post bacterial challenge.

3.5 Thickness distribution over the RWM surface

The thickness data (mean values with SDs) measured at all seven locations across the RWM surface from both uninfected and infected chinchillas are displayed in Fig. 7 and listed in Table 1. The results show that the thickness of RWM in normal or uninfected ears was not uniformly distributed over the membrane. The RWM was thicker in the boundary region with an average of 15 μm compared to that in the central region of about 12~13 μm. AOM resulted in a significant increase of the RWM thickness in the central area and boundary region. At other locations, the change of RWM thickness such as along the lateral to medial (locations L and M) was observed, but not statistically significant (Table 1).

Moreover, the results from the present study in Fig. 7 show that there were no significant thickness changes between two AOM phases, 4 days vs. 8 days post bacterial challenge, at most locations across the RWM. This suggests that *H. influenzae*-induced AOM 4 to 8 days may not produce more severe structural changes of this type in the RWM over the full course of the middle ear infection. Future full term (duration 30 days) infection studies of AOM are planned to address this issue.

4. DISCUSSION

4.1 H. influenzae induced AOM and tissue morphological changes

The chinchilla model of AOM produced by transbullar injection of *H. influenzae* strain 86-028NP has been widely used for various research purposes [12, 13, 26–30]. Recently we used this AOM model to identify biomechanical changes in hearing associated with the effects of acute infection on the tympanic membrane [13, 30]. In the present study, we utilized this model to assess the early acute impact (days 4 and 8 post bacterial challenge) of this *H. influenzae* strain on RWM histopathological changes. Consistent accumulation of a measureable amount of middle ear effusion in response to such an infection occurred by day 4 post infection. Bacterial titers (~1× 10^8 cfu per ml middle ear fluid) typically remain comparable between days 4 and 8 and do so for approximately an additional two weeks [28]. Within four days of infection of the middle ear, a statistically significant, 2–3 μm increase in RWM thickness was observed in each of the infected chinchillas in the present study. These thickness increases occurred at all RWM locations except at its lateral and medial areas. After AOM of 8 days duration, thickness of the RWM remained essentially unchanged compared to that found in chinchillas infected for 4 days.

To explain the observation of thickness change at the medial and lateral areas not statistically significant may need further study by increasing the sample size for thickness measurement. The mean values of the RWM thickness at L and M locations listed in Table 1 or Fig. 7 show some difference among the control, 4D, and 8D ears, but the relatively large standard deviation made the statistical results not significant. Another concern is the possible artifact of the processing method. The histologic images on the central line (P1, P2, A1, A2 and O) for each specimen were captured and measured from a single section along

the long axis of the RWM. The thicknesses at L and M were measured from different sections. Even though all the sections were supposed to be made in the same direction perpendicular to the surface of the membrane and parallel to the central line, the errors probably occurred and the sections were not processed in the exactly same manner. This could also be related to the large standard deviations at L and M.

Interestingly, these RWM thickness changes differed from the TM thickness changes we recently described in this chinchilla AOM model [13] even though the RWM and the TM are both soft membrane tissues with a multi-layer structure. The continued significant increase in TM thickness between days 4 and 8 post *H. influenzae* infection was not observed in the RWM. A possible explanation for this difference in response between these two middle ear membranes is that although cell infiltration, intracellular edema and cell proliferation occur concomitantly in the RWM and the TM, contact of their membrane surfaces with the middle ear effusion differs between these two membranes. The RWM is protected by the round window niche and sometimes partially covered by the false RWM [4], while the TM is in direct contact with middle ear effusions.

A second possible explanation for this observed structural difference between these two membranes is attributable to cell proliferation in the TM epidermal layer. While cellular proliferation occurs on both sides of the TM [13], this bilateral effect appears not to occur in the RWM. The outer epithelial layer of the RWM proliferated to a lesser degree and remained unstratified after infection. The fibrous layer of the RWM also does not have two distinct and orthogonal fiber layers like the TM although both radial and circumferential fiber bundles have been observed in its connective tissue layer [4]. Stratification of the TM fibrous interlayer potentially provides space for greater edema in the TM than in the RWM. Taken together, these observations suggest that different soft tissues of the middle ear have distinct, non-identical inflammatory responses because of their specialized structural features.

Chinchilla RWM thickness has been measured under normal (uninfected) and different diseased conditions. Schachern et al. [20] reported that the normal chinchilla RWM thickness was 13.7 ± 2.9 μm, a value consistent with our control group results recorded in Table 1. The thickness of pneumococcal surface protein A mutant and pneumococcal surface antigen A mutant treated RWM was approximately 15–20 μm [22]. Their result was comparable to our data from the infected groups. A later report by Schachern et al. [23] using the *H. influenzae* strain 2019 (0.5 ml of 10^2 CFU/ml) showed that the average RWM thickness reached 42 μm two days post inoculation with severe infection inside the cochlea. This thickness change is higher than what we observed in the present study. The difference of RWM thickness measured after bacterial challenge may be related to different bacterial strain as well as the time course of infection. Strain-specific differences in the severity of these pathological changes deserves further characterization in future studies.

Moreover, an important earlier study by Schachern et al. [19] identified that staphylococcal exotoxin can induced changes in the chinchilla RWM, which are similar to those we found after *H. influenzae* infection. Overall, the microstructural alternations induced by staphylococcal exotoxin appear rather similar to those associated with *H. influenzae*

infection. Epithelial cell proliferation, alteration of the RWM surface, inflammatory cell infiltration, and intracellular edema were identified in both their and our studies. The severity of the inflammation we observed in the RWM after infection for 4 or 8 days was comparable to the effect of seven daily injections of exotoxin in this early study. The exact mechanisms causing these effects are complex, currently unknown in *H. influenzae*, and may or may not be similar.

Histologic results also show that the curved shape of the RWM cross section varied in both 4 day and 8 day AOM (see Fig. 2). The cross sections of the RWM, which suppose to have a smooth concave shape in normal ear showed some local changes of curvature after the infection was induced. This observation may indicate that membrane tension was reduced at both 4 and 8 days post infection. One explanation for this RWM shape change is the occurrence of material properties changes of the RWM caused by AOM. The decreased stiffness of RWM tissue may also result from the cellular infiltration and edema as we have previously reported for the chinchilla [6] and guinea pig [7] model of AOM. Another possible explanation for this occurrence is negative middle ear pressure is generated during the AOM disease course [12]. Thus, both pressure differences across the RWM and material changes may cause the slack, irregular shape of RWM shown in Fig. 2.

4.2 Contribution of this work

Previous studies from our laboratory established that negative middle ear pressure, middle ear effusion and soft tissue structural changes are three major factors induced by AOM that are directly associated with conductive hearing loss [10, 12]. AOM-associated thickness alterations and microstructural changes can alter the ear's mechanical properties and this leads to impaired hearing. However, although the chinchilla is a widely used experimental animal in hearing research, the quantitative description of RWM thickness distribution across the entire surface here-to-fore has been quite limited in both normal and AOM animals. The present study provides a detailed set of quantitative information on morphological changes of the RWM in ears with acute *H. influenzae*-induced AOM. Interestingly, it was found that the thickness change of RWM from the 4 days to 8 days post infection was different from that of the TM. Our findings suggest that morphological change of ear tissue over the infection course vary with the anatomy and function of the specific tissue in the ear.

Moreover, the simplified geometry model of RWM with uniform or centrally-symmetric thickness distribution has been used for characterizing mechanical properties of the RWM in otitis media. The thickness distribution of RWM across the entire surface reported in this study is expected to provide useful data to improve the accuracy of modeling the RWM, for determining its mechanical properties, and for improving our understanding the RWM's mechanistic role in sound transmission into the cochlea.

5. CONCLUSIONS

Our present study quantitatively describes the complex pathological changes occurring in the chinchilla round window membrane following middle ear infection by a clinical isolate of nontypeable *Haemophilus influenzae.* RWM structure and thickness in chinchilla ears were

characterized histologically during the early course of acute otitis media (4 and 8 days post bacterial challenge). Thickness of the RWM along the central line increased (by 2~3 μm) in a statistically significant manner by 4 days post challenge. Such thickness changes did not occur in the lateral and medial areas of the RWM. Three major contributors to the observed thickness increases were proliferation of epithelial cells, infiltration of inflammatory cells and intracellular edema. Neither additional alterations in RWM structure, nor statistically significant differences in severity of the pathological changes, were observed at 8 days after infection. Our laboratory has now established that both the tympanic membrane and the round window membrane of the chinchilla exhibit pathological changes associated with *H. influenzae*-induced otitis media. Taken together, these findings imply that otitis media induced by notypeable *H. influenzae* can directly affect sound transmission into the cochlea via its acute pathological effects on both the tympanic membrane and the round window. We plan to delineate further the complete time course of these pathological effects, their repair, and their prevention, in future studies for our laboratory.

Acknowledgments

We thank Dr. Xiying Guan for his help in sample preparation and Hitt Brooke for her dedicated data analyses. This study was supported by NIH grant R01DC011585.

References

1. Wever EG, Lawrence M. The functions of the round window. Ann Otol Rhinol Laryngol. 1948; 57:579–589. [PubMed: 18885439]
2. Goycoolea MV, Muchow D, Schachern P. Experimental studies on round window structure: function and permeability. Laryngoscope. 1988; 98:1–20. [PubMed: 3287079]
3. Goycoolea MV, Lundman L. Round window membrane. Structure function and permeability: A review. Microsc Res Tech. 1997; 36:201–211. [PubMed: 9080410]
4. Goycoolea MV. Clinical aspects of round window membrane permeability under normal and pathological conditions. Acta Otolaryngol. 2001; 121:437–447. [PubMed: 11508501]
5. Juhn SK, Hamaguchi Y, Goycoolea MV. Review of round window membrane permeability. Acta Otolaryngol. 1988; 105:43–48.
6. Wang X, Nakmali D, Gan RZ. Complex modulus of round window membrane over auditory frequencies in normal and otitis media chinchilla ears. Int J Exp Comput Biomech. 2015; 3:27–44.
7. Gan RZ, Nakmali D, Zhang X. Dynamic properties of round window membrane in guinea pig otitis media model measured with electromagnetic stimulation. Hear Res. 2013; 301:125–136. [PubMed: 23333258]
8. Cureoglu S, Schachern P, Rinaldo A, Tsuprun V, Ferlito A, Paparella M. Round window membrane and labyrinthine pathological changes: An overview. Acta Otolaryngol. 2005; 125:9–15. [PubMed: 15799567]
9. Dai C, Gan RZ. Change of middle ear transfer function in otitis media with effusion model of guinea pigs. Hear Res. 2008; 243:78–86. [PubMed: 18586077]
10. Guan X, Gan RZ. Mechanisms of tympanic membrane and incus mobility loss in acute otitis media model of guinea pig. J Assoc Res Otolaryngol. 2013; 14:295–307. [PubMed: 23483330]
11. Guan X, Li W, Gan RZ. Comparison of eardrum mobility in acute otitis media and otitis media with effusion models. Otol Neurotol. 2013; 34:1316–1320. [PubMed: 23921936]
12. Guan X, Chen Y, Gan RZ. Factors affecting loss of tympanic membrane mobility in acute otitis media model of chinchilla. Hear Res. 2014; 309:136–146. [PubMed: 24406734]
13. Guan X, Jiang S, Seale TW, Hitt BM, Gan RZ. Morphological changes in the tympanic membrane associated with Haemophilus influenzae-induced acute otitis media in the chinchilla. Int J Pediatr Otorhinolaryngol. 2015; 79:1462–1471. [PubMed: 26183006]

14. Sahni RS, Paparella MM, Schachern PA, Goycoolea MV, Le CT. Thickness of the human round window membrane in different forms of otitis media. Arch Otolaryngol Head Neck Surg. 1987; 113:630–634. [PubMed: 3566946]
15. Joglekar S, Morita N, Cureoglu S, Schachern P, Deroee A, Tsuprun V. Cochlear pathology in human temporal bones with otitis media. Acta Otolaryngol. 2010; 130:472–476. [PubMed: 19895333]
16. Goycoolea MV, Paparella MM, Carpenter AM, Juhn SK. Oval and round window changes in otitis media: An experimental study in the cat. Surg Forum. 1977; 29:578–580. [PubMed: 401269]
17. Goycoolea MV, Paparella MM, Goldberg B, Carpenter A. Permeability of the round window membrane in otitis media. Arch Otolaryngol. 1980; 106:430–433. [PubMed: 7387533]
18. Ikeda K, Morizono T, Takasaka T. Otic Preparations altered permeability and thickness of the round window membrane of the chinchilla. ORL. 1991; 53:91–93. [PubMed: 2011381]
19. Schachern PA, Paparella MM, Goycoolea M, Goldberg B, Schlievert P. The round window membrane following application of staphylococcal exotoxin: An electron microscopic study. Laryngoscope. 1981; 91:2007–2017. [PubMed: 7321721]
20. Schachern PA, Paparella MM, Duvall AJ III. The normal chinchilla round window membrane. Arch Otolaryngol. 1982; 108:550–554. [PubMed: 7115183]
21. Schachern PA, Paparella MM, Goycoolea MV, Duvall AJ III, Choo Y. The permeability of the round window membrane during otitis media. Arch Otolaryngol Head Neck Surg. 1987; 113:625–629. [PubMed: 3566945]
22. Schachern P, Tsuprun V, Cureoglu S, Ferrieri P, Briles D, Paparella M. The round window membrane in otitis media: effect of pneumococcal proteins. Arch Otolaryngol Head Neck Surg. 2008; 134:658–662. [PubMed: 18559736]
23. Schachern PA, Tsuprun V, Wang B, Apicella MA, Cureoglu S, Paparella MM. Effect of lipooligosaccharide mutations of Haemophilus influenzae on the middle and inner ears. Int J Pediatr Otorhinolaryngol. 2009; 73:1757–1760. [PubMed: 19853312]
24. Nomura Y. Otological significance of the round window. Adv Otorhinolaryngol. 1983; 33:1–162. [PubMed: 6377855]
25. Kim CS, Cho TK, Jinn TH. Permeability of the round window membrane to horseradish peroxidase in experimental otitis media. Otolaryngol Head Neck Surg. 1990; 103:918–925. [PubMed: 2126126]
26. Morton DJ, Hempel RJ, Seale TW, Whitby PW, Stull TL. A functional tonB gene is required for both virulence and competitive fitness in a chinchilla model of Haemophilus influenzae otitis media. BMC Res Notes. 2012; 5:327. [PubMed: 22731867]
27. Bakaletz LO, Kennedy BJ, Novotny LA, Duquesne G, Cohen J, Lobet Y. Protection against development of otitis media induced by nontypeable Haemophilus influenzae by both active and passive immunization in a chinchilla model of virus-bacterium superinfection. Infect Immun. 1999; 67:2746–2762. [PubMed: 10338477]
28. Morton DJ, Bakaletz LO, Jurcisek JA, VanWagoner TM, Seale TW, Whitby PW. Reduced severity of middle ear infection caused by nontypeable Haemophilus influenzae lacking the hemoglobin/hemoglobin–haptoglobin binding proteins (Hgp) in a chinchilla model of otitis media. Microb Pathog. 2004; 36:25–33. [PubMed: 14643637]
29. Mason KM, Munson RS Jr, Bakaletz LO. Nontypeable Haemophilus influenzae gene expression induced in vivo in a chinchilla model of otitis media. Infect Immun. 2003; 71:3454–3462. [PubMed: 12761130]
30. Yokell Z, Wang X, Gan RZ. Dynamic properties of tympanic membrane in a chinchilla otitis media model measured with acoustic loading. J Biomech Eng. 2015; 137 081006-1 to -9.

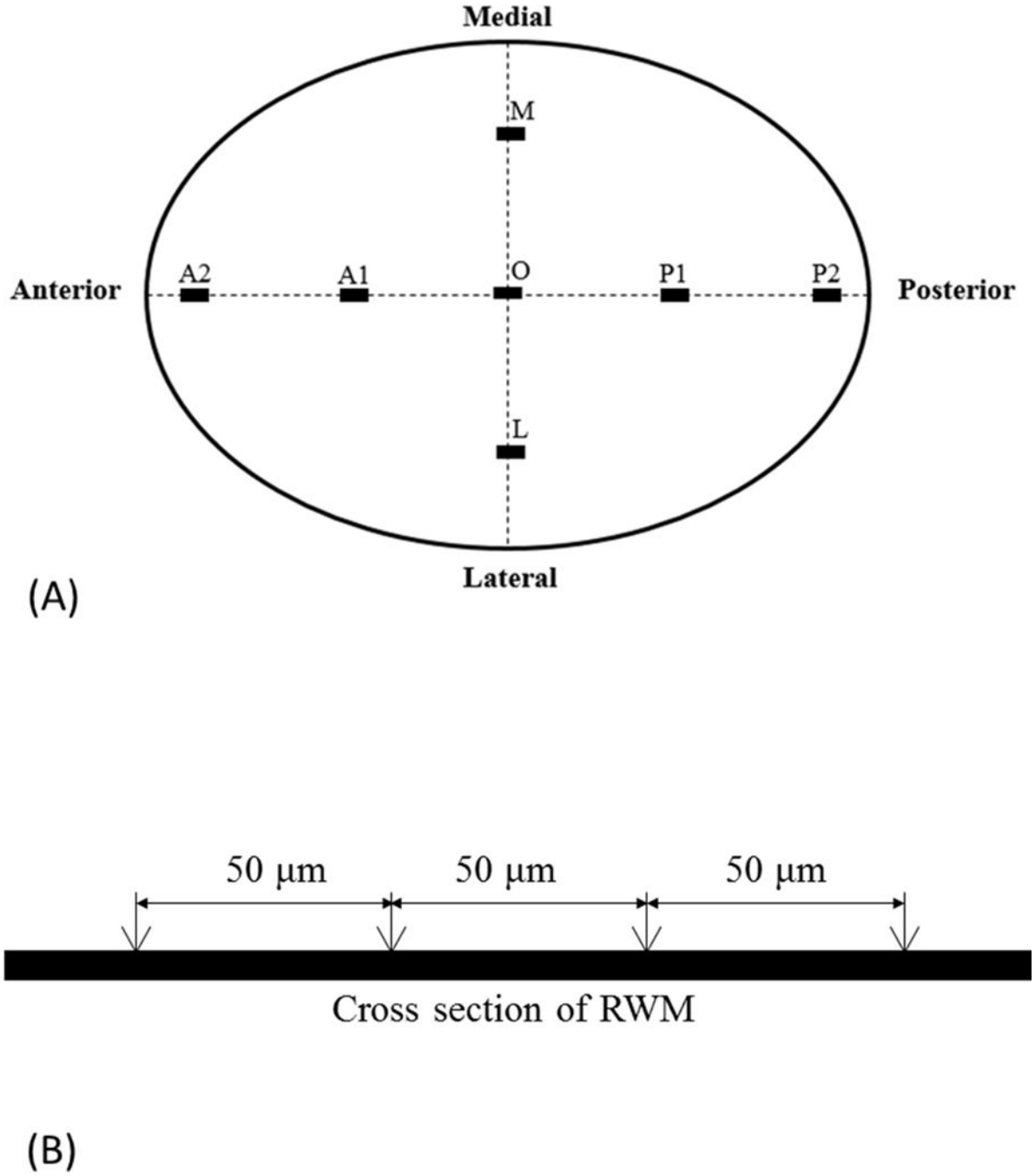

Figure 1.

(A) Schematic representation of histologic sectioning of the RWM. Thickness measurements were made at seven locations in each RWM specimen. (B) A schematic drawing showing that the thickness of the RWM at each location was obtained by averaging the thickness measured at four points about 50 μm away from each other.

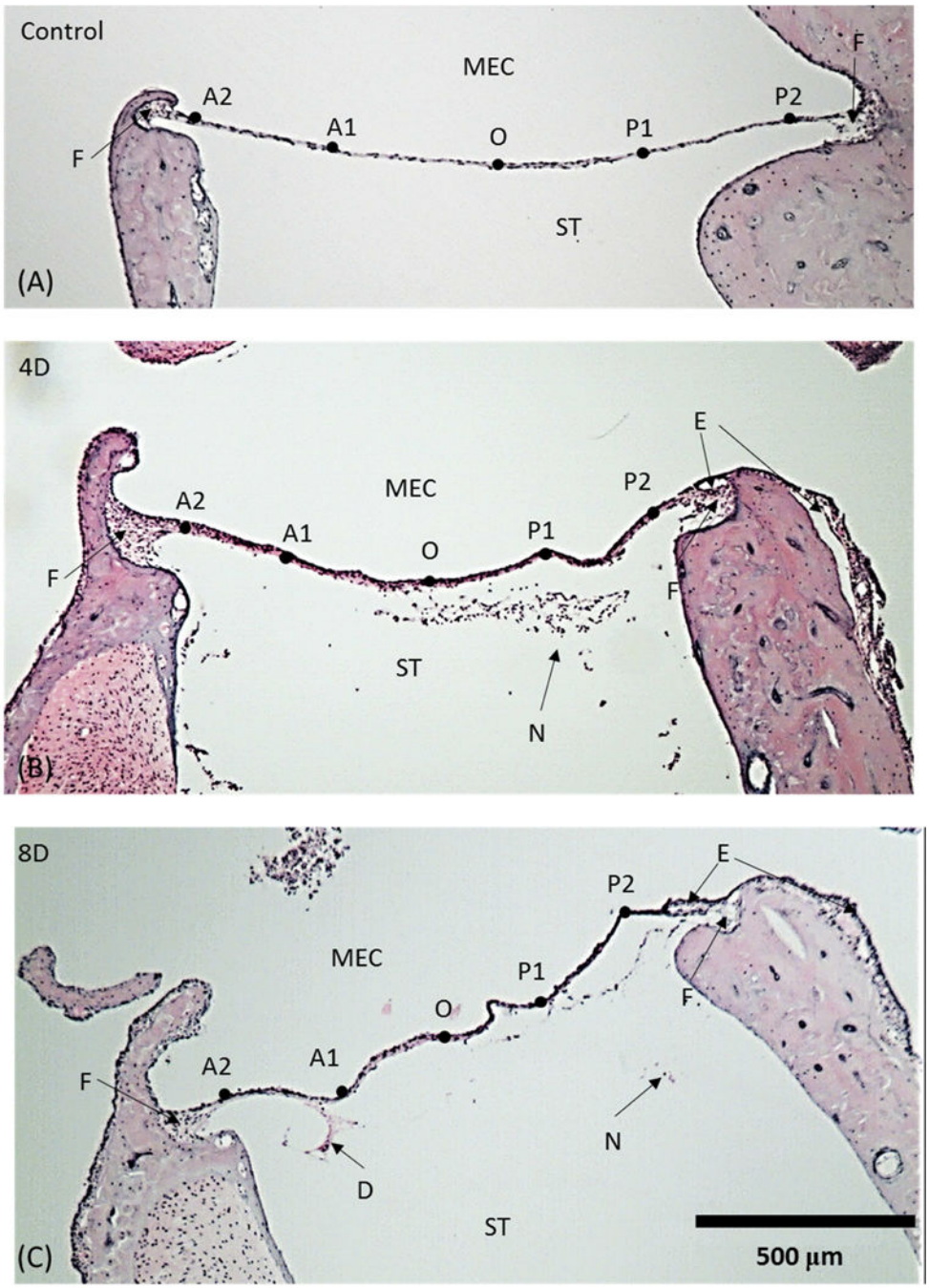

Figure 2.

Representative histologic images of the RWM along the long axis. Five selected locations are labeled as A2, A1, O, P1 and P2. (A) control (uninfected) ear; (B) 4 day (4D) infected AOM ear; (C) 8 day (8D) infected AOM ear; ST, scala tympani; MEC, middle ear cavity; N, neutrophil; E, edema; D, desquamation; F, fan -shape area.

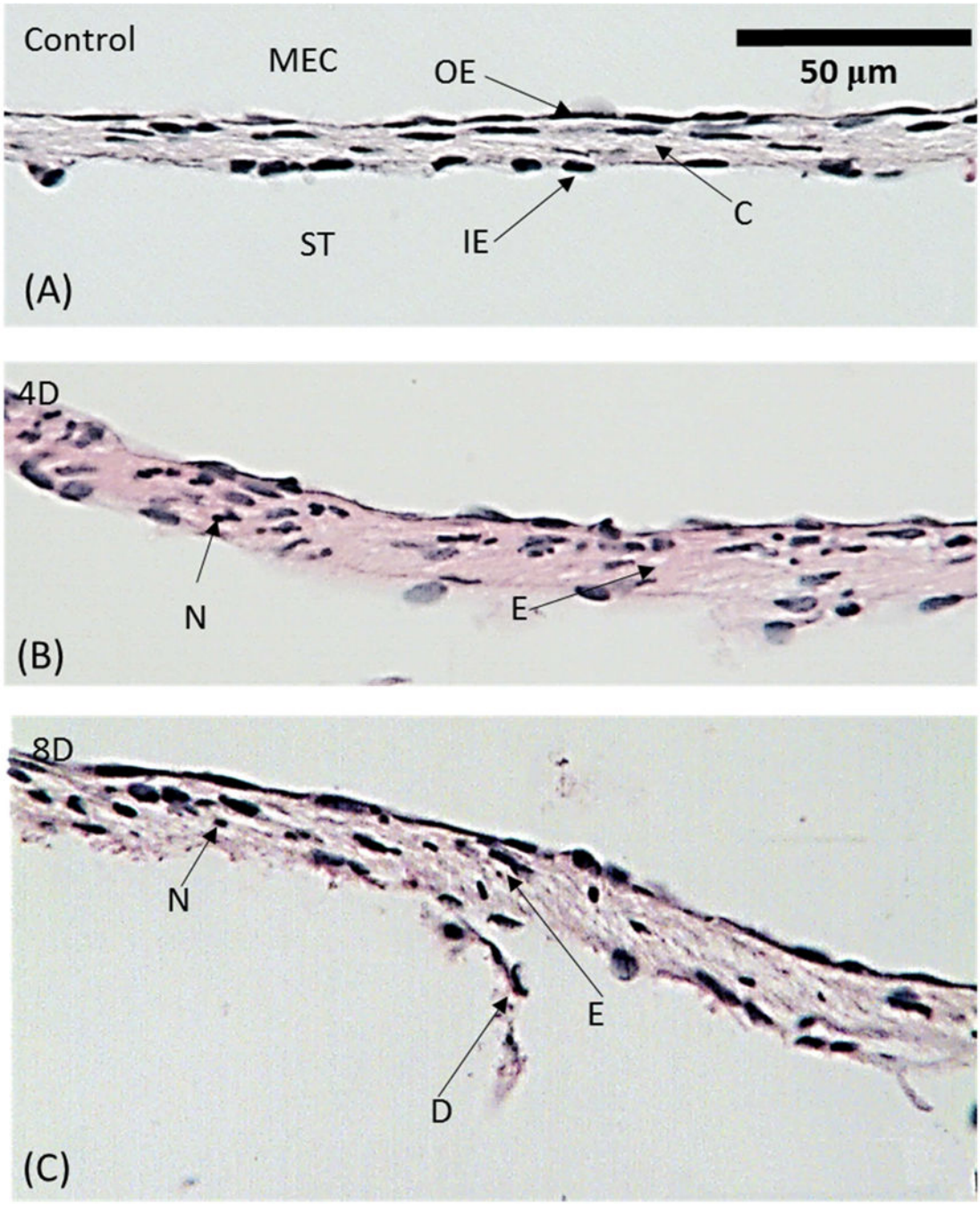

Figure 3.

Histologic images of representative RWMs taken at the center O. (A) control (uninfected) ear; (B) 4D infected ear; (C) 8D infected ear. ST, scala tympani; MEC, middle ear cavity; OE, outer epithelium layer; IE, inner epithelium layer; C, connective tissue layer; D, desquamation; N, neutrophil; E, edema.

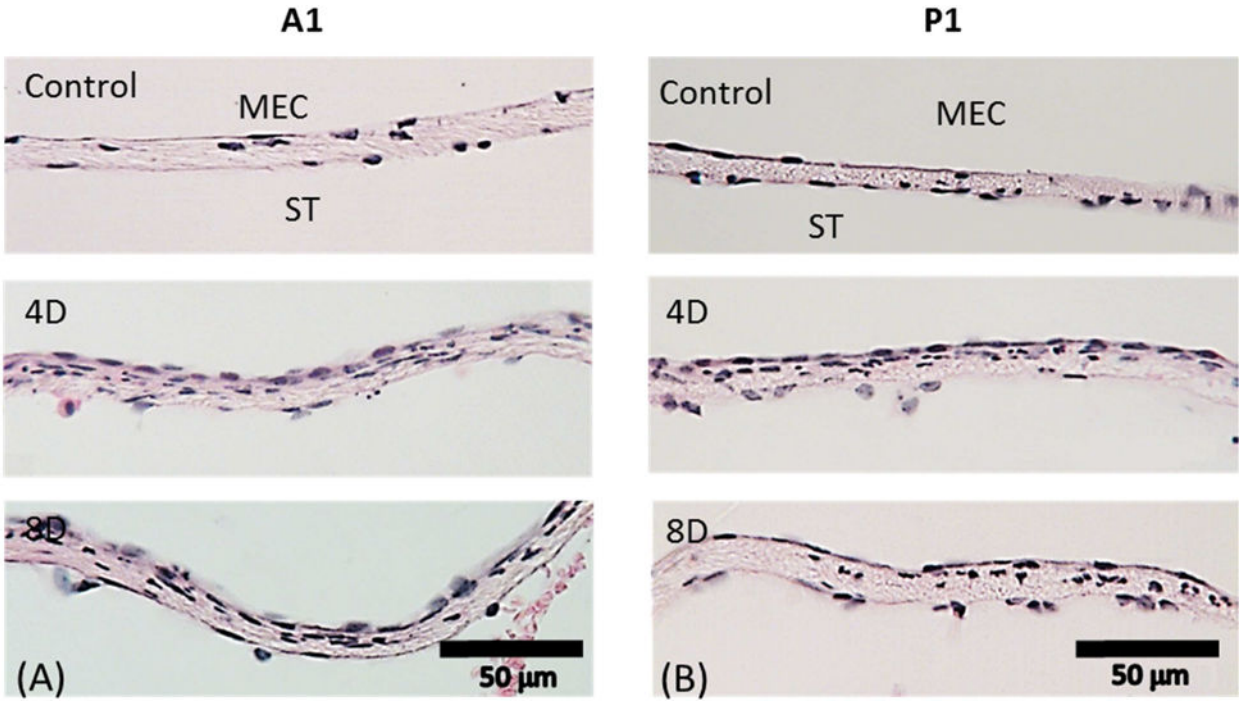

Figure 4.

Representative histologic images taken at (A) A1; (B) P1. The upper panels show representative RWMs from control ears. The middle panels show representatives of 4D RWMs. The lower panels show representatives of 8D RWMs. ST, scala tympani; MEC, middle ear cavity.

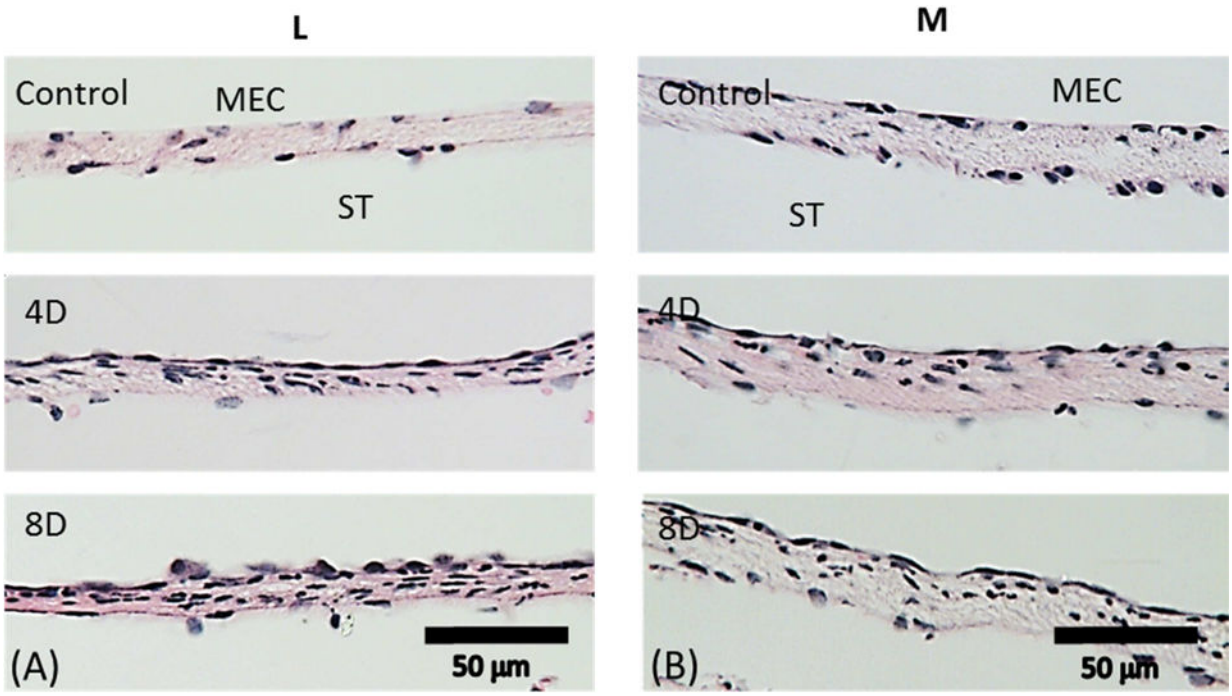

Figure 5.

Representative histologic images taken at (A) L; (B) M. The upper panels are from control ears. The middle panels are from 4D ears. The lower panels are from 8D ears. ST, scala tympani; MEC, middle ear cavity.

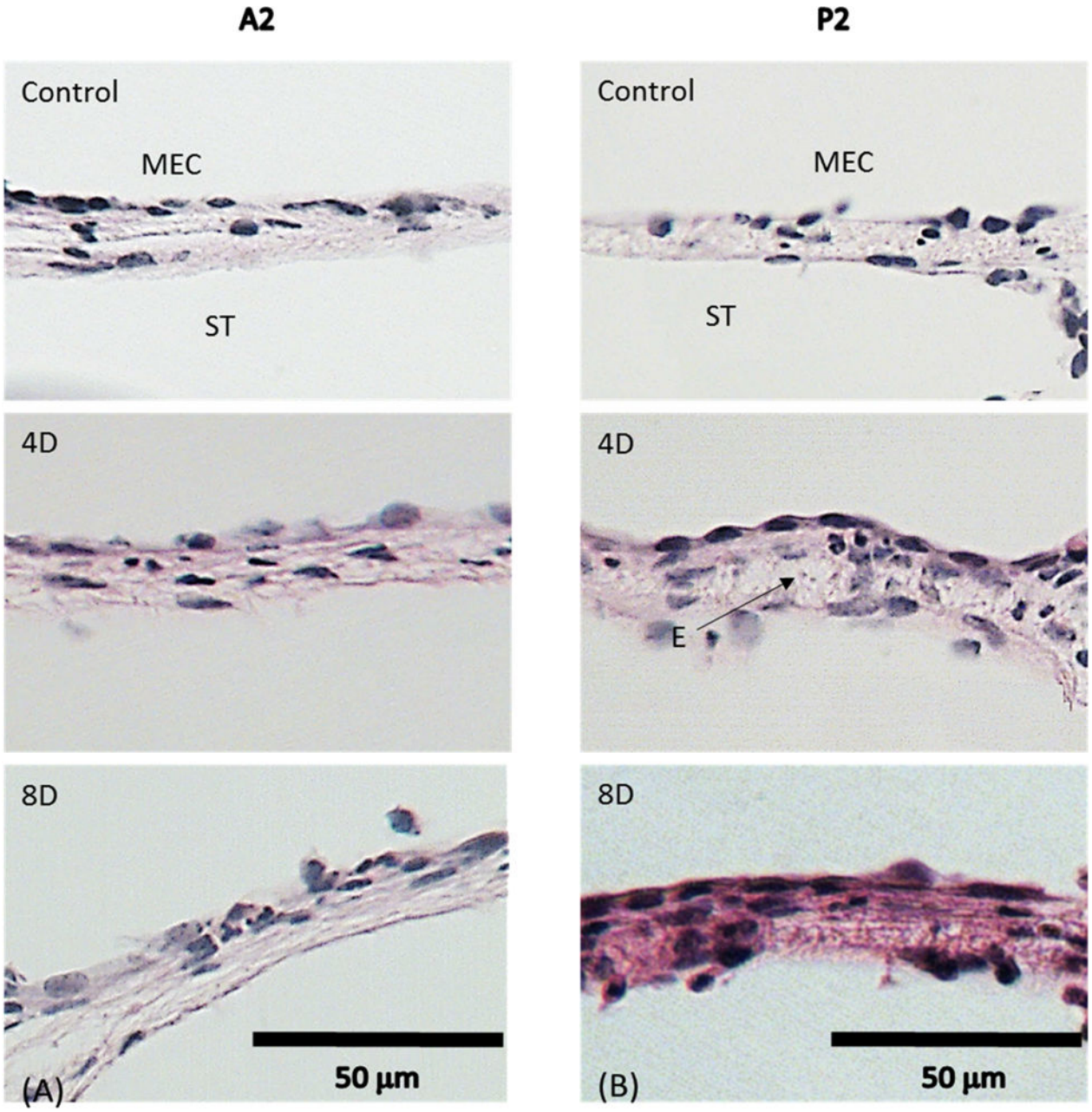

Figure 6.

Representative histologic images taken at (A) A2; (B) P2. The upper panels are from control ears. The middle panels are from 4D ears. The lower panels are from 8D ears. ST, scala tympani; MEC, middle ear cavity; E, edema.

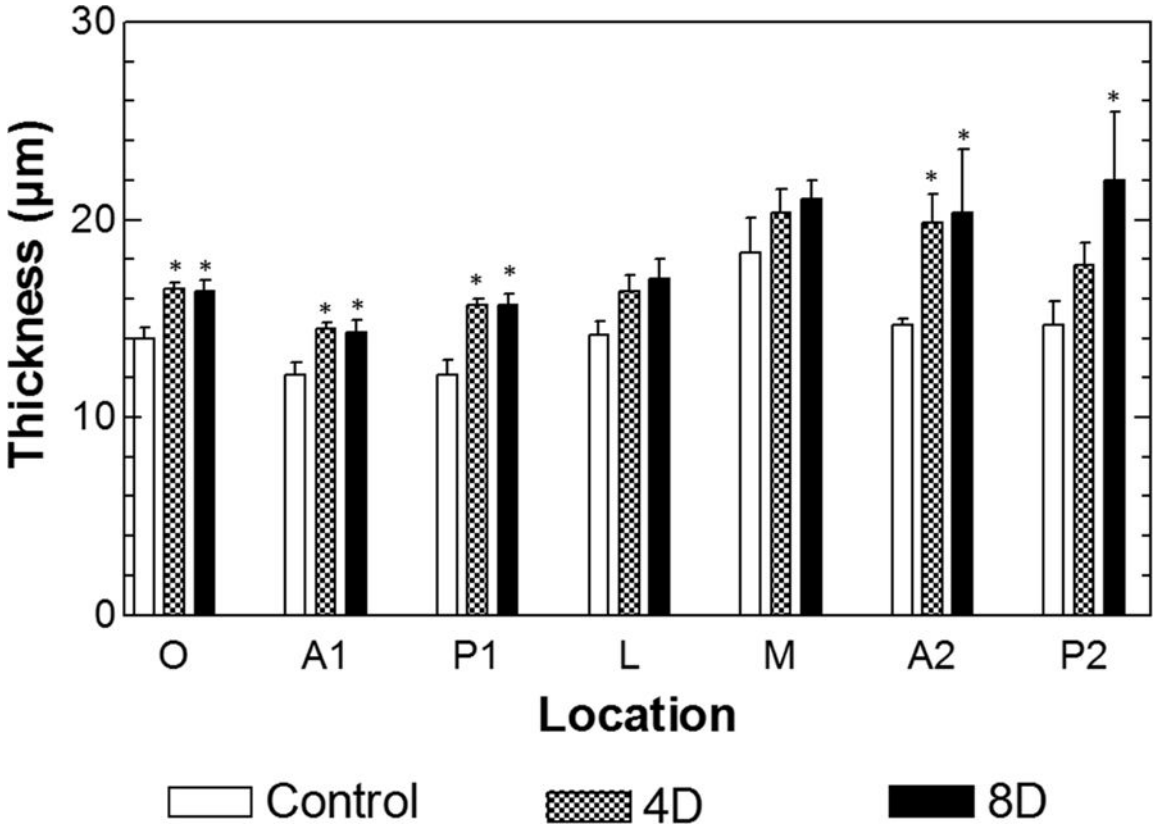

Figure 7.

Distribution of the RWM thickness with mean and SD from 7 locations across the surface in control, 4D, and 8D ears. Asterisk symbols are used to highlight data group with statistically significant differences comparing to the uninfected controls.

Table 1

Mean thickness of the round window membrane with standard deviation at 7 locations along the central line in control, 4 day (4D), and 8 day (8D) AOM ears with the unit of μm (N=3 for each group).

	Control	4D	8D
O	14.00 ± 1.00	16.50 ± 0.50*	16.30 ± 0.58*
A1	12.20 ± 1.04	14.50 ± 0.50*	14.30 ± 0.58*
P1	12.20 ± 1.26	15.70 ± 0.58*	15.70 ± 0.58*
L	14.20 ± 1.26	16.30 ± 1.53	17.00 ± 1.00
M	18.30 ± 3.06	20.30 ± 2.08	21.00 ± 1.00
A2	14.70 ± 0.58	19.80 ± 2.57*	20.30 ± 3.21*
P2	14.70 ± 2.08	17.70 ± 2.08	22.00 ± 3.46*

Note: Asterisk symbols are used to highlight data group with statistically significant differences comparing to the uninfected controls.